Time-Reversal Symmetry Breaking in Re-Based Superconductors

T. Shang,[1,2,3,*] M. Smidman,[4,†] S. K. Ghosh,[5] C. Baines,[6] L. J. Chang,[7] D. J. Gawryluk,[1,‖] J. A. T. Barker,[6] R. P. Singh,[8] D. McK. Paul,[9] G. Balakrishnan,[9] E. Pomjakushina,[1] M. Shi,[2] M. Medarde,[1] A. D. Hillier,[10] H. Q. Yuan,[4,11] J. Quintanilla,[5,‡] J. Mesot,[12,3,13] and T. Shiroka[13,12,§]

[1]*Laboratory for Multiscale Materials Experiments, Paul Scherrer Institut, Villigen CH-5232, Switzerland*
[2]*Swiss Light Source, Paul Scherrer Institut, Villigen CH-5232, Switzerland*
[3]*Institute of Condensed Matter Physics, École Polytechnique Fédérale de Lausanne (EPFL), Lausanne CH-1015, Switzerland*
[4]*Center for Correlated Matter and Department of Physics, Zhejiang University, Hangzhou 310058, China*
[5]*School of Physical Sciences, University of Kent, Canterbury CT2 7NH, United Kingdom*
[6]*Laboratory for Muon-Spin Spectroscopy, Paul Scherrer Institut, CH-5232 Villigen PSI, Switzerland*
[7]*Department of Physics, National Cheng Kung University, Tainan 70101, Taiwan*
[8]*Indian Institute of Science Education and Research Bhopal, Bhopal, 462066, India*
[9]*Physics Department, University of Warwick, Coventry CV4 7AL, United Kingdom*
[10]*ISIS Facility, STFC Rutherford Appleton Laboratory, Harwell Science and Innovation Campus, Oxfordshire, OX11 0QX, United Kingdom*
[11]*Collaborative Innovation Center of Advanced Microstructures, Nanjing Univeristy, Nanjing 210093, China*
[12]*Paul Scherrer Institut, CH-5232 Villigen PSI, Switzerland*
[13]*Laboratorium für Festkörperphysik, ETH Zürich, CH-8093 Zurich, Switzerland*

(Received 11 March 2018; revised manuscript received 30 July 2018; published 21 December 2018)

To trace the origin of time-reversal symmetry breaking (TRSB) in Re-based superconductors, we performed comparative muon-spin rotation and relaxation (μSR) studies of superconducting noncentrosymmetric $Re_{0.82}Nb_{0.18}$ ($T_c = 8.8$ K) and centrosymmetric Re ($T_c = 2.7$ K). In $Re_{0.82}Nb_{0.18}$, the low–temperature superfluid density and the electronic specific heat evidence a fully gapped superconducting state, whose enhanced gap magnitude and specific-heat discontinuity suggest a moderately strong electron-phonon coupling. In both $Re_{0.82}Nb_{0.18}$ and pure Re, the spontaneous magnetic fields revealed by zero-field μSR below T_c indicate time-reversal symmetry breaking and thus unconventional superconductivity. The concomitant occurrence of TRSB in centrosymmetric Re and noncentrosymmetric ReT (T = transition metal), yet its preservation in the isostructural noncentrosymmetric superconductors $Mg_{10}Ir_{19}B_{16}$ and $Nb_{0.5}Os_{0.5}$, strongly suggests that the local electronic structure of Re is crucial for understanding the TRSB superconducting state in Re and ReT. We discuss the superconducting order parameter symmetries that are compatible with the experimental observations.

DOI: 10.1103/PhysRevLett.121.257002

Time reversal and spatial inversion are two key symmetries that influence, at a fundamental level, the electron pairing in the superconducting state. On the one hand, a number of unconventional superconductors exhibit spontaneous time-reversal symmetry breaking (TRSB) on entering the superconducting state; on the other hand, the absence of inversion symmetry already above T_c leads to an antisymmetric spin-orbit coupling (SOC), lifting the degeneracy of the conduction-band electrons and potentially giving rise to a mixed-parity superconducting state [1,2]. Some noncentrosymmetric superconductors (NCSC), such as $CePt_3Si$ [3], $CeIrSi_3$ [4], Li_2Pt_3B [5,6], and $K_2Cr_3As_3$ [7,8], exhibit line nodes in the gap, while others, such as $LaNiC_2$ [9] and $(La, Y)_2C_3$ [10], show multiple nodeless superconducting gaps. In addition, due to the strong influence of SOC, their upper critical field can greatly exceed the Pauli limit, as has been found in $CePt_3Si$ [11] and very recently in $(Ta, Nb)Rh_2B_2$ [12].

In general, TRSB below T_c and a lack of spatial-inversion symmetry of the crystal structure are independent events. Yet, in a few cases, such as in $LaNiC_2$ [13], La_7Ir_3 [14], and in particular, in the Re-based compounds Re_6Zr [15], Re_6Hf [16], Re_6Ti [17], and $Re_{24}Ti_5$ [18], TRSB below T_c is concomitant with an existing lack of crystal inversion symmetry. Such an unusually frequent occurrence of TRSB among the superconducting ReT binary alloys (T = transition metal) is rather puzzling. Its persistence, independent of the particular transition metal, points to a key role played by Re. To test such a hypothesis, and to ascertain the possible relevance of the noncentrosymmetric structure to TRSB in Re-based NCSC, we proceeded with a twofold study. On one hand, we synthesized and investigated another Re-based NCSC, $Re_{0.82}Nb_{0.18}$. On the other hand, we considered the pure Re metal, also a superconductor, but with a centrosymmetric structure.

A comparative study by means of muon-spin relaxation and rotation (μSR) allows us to address the question of TRSB in Re-containing compounds. The choice of μSR as the preferred technique for our study is justified by its key role in detecting TRSB in numerous unconventional superconductors [13–20] (later confirmed by the Kerr effect or bulk magnetization in the cases of Sr_2RuO_4, UPt_3, and $LaNiC_2$ [21–23]). We report systematic μSR studies of $Re_{0.82}Nb_{0.18}$ ($T_c = 8.8$ K) and Re ($T_c = 2.7$ K), whose bulk superconducting properties were characterized by magnetic, transport, and thermodynamic measurements. The μSR data show that spontaneous magnetic fields appear below the respective transition temperatures, thus implying that the superconducting states of both $Re_{0.82}Nb_{0.18}$ and Re show TRSB and have an unconventional nature. Since pure Re is centrosymmetric, this implies that the noncentrosymmetric structure is not a requirement for TRSB in these materials.

Polycrystalline $Re_{0.82}Nb_{0.18}$ samples were prepared by arc melting Re and Nb metals and the same Re powder was used for measurements on elementary Re. The x-ray powder diffraction measured using a Bruker D8 diffractometer, confirmed the α-Mn structure of $Re_{0.82}Nb_{0.18}$ ($I\bar{4}3m$) and the hcp-Mg structure of Re ($P6_3/mmc$) [24–30]. Magnetic susceptibility, electrical resistivity, and specific-heat measurements were performed on a 7-T Quantum Design Magnetic Property Measurement System and a 9-T Physical Property Measurement System. The μSR measurements were carried out on both the MuSR instrument of the ISIS pulsed muon source (UK) [31], and the GPS and LTF spectrometers of the πM3 beam line at the Paul Scherrer Institut, Villigen, Switzerland.

The magnetic susceptibility was determined using both field-cooled (FC) and zero-field-cooled (ZFC) protocols. As shown in Figs. 1(a)–1(b), the splitting of the two curves is typical of type-II superconductors, with the ZFC-susceptibility indicating bulk superconductivity with $T_c = 8.8$ K for $Re_{0.82}Nb_{0.18}$ and 2.7 K for Re. The bulk superconductivity of $Re_{0.82}Nb_{0.18}$ was further confirmed by electrical resistivity and specific-heat data [24]. To perform transverse-field muon-spin rotation (TF-μSR) measurements of superconductors, the applied field should exceed the lower critical field $\mu_0 H_{c1}$, so that the additional field-distribution broadening, due to the flux-line lattice (FLL), can be determined from the decay of the μSR asymmetry. To determine $\mu_0 H_{c1}$, the field-dependent magnetization $M(H)$ was measured at various temperatures below T_c, as shown in Fig. 1(c), for $Re_{0.82}Nb_{0.18}$ [for $M(H)$ data of Re, see Supplemental Material] [24]. The derived $\mu_0 H_{c1}$ values are plotted in Fig. 1(d) as a function of temperature. The dashed lines are fits to $\mu_0 H_{c1}(T) = \mu_0 H_{c1}(0)[1-(T/T_c)^2]$, which yield estimates of lower critical fields of 6.4(1) mT and 3.7(2) mT in $Re_{0.82}Nb_{0.18}$ and Re, respectively.

The TF-μSR measurements allowed us to explore the nature of superconductivity in $Re_{0.82}Nb_{0.18}$ at a microscopic level. The optimal field value for such experiments (above H_{c1}) was determined via preliminary field-dependent μSR measurements at 1.5 K [24]. Figure 2(a) shows two representative TF-μSR spectra collected above and below T_c in an applied field of 15 mT. In the superconducting mixed state, the faster decay of muon-spin polarization reflects the inhomogeneous field distribution due to the FLL. The corresponding TF spectra are described by:

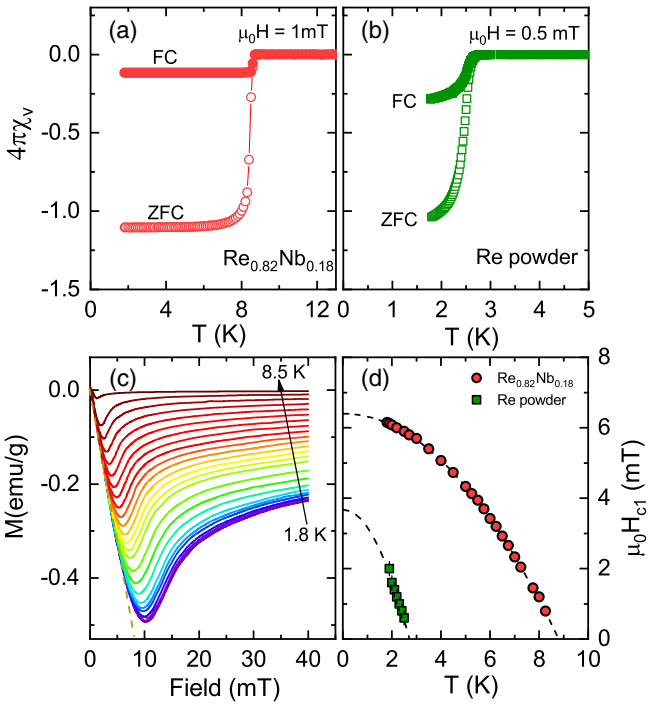

FIG. 1. Temperature-dependent magnetic susceptibilities of (a) $Re_{0.82}Nb_{0.18}$, and (b) pure Re, measured at 1 mT and 0.5 mT, respectively. (c) Magnetization vs applied magnetic field recorded at different temperatures up to T_c for $Re_{0.82}Nb_{0.18}$. For each temperature, $\mu_0 H_{c1}$ was determined from the value where $M(H)$ deviates from linearity (see dashed line). (d) $\mu_0 H_{c1}$ vs temperature for both samples; dashed lines represent fits to $\mu_0 H_{c1}(T) = \mu_0 H_{c1}(0)[1-(T/T_c)^2]$.

$$P_{\mathrm{TF}} = P_s \cos(\gamma_\mu B_s t + \phi) e^{-\sigma^2 t^2/2} + P_{\mathrm{bg}} \cos(\gamma_\mu B_{\mathrm{bg}} t + \phi).$$

Here, P_s and P_{bg} represent the muon-spin polarization for muons implanted in the sample and sample holder, respectively, with the latter not undergoing any depolarization. $\gamma_\mu = 2\pi \times 135.53$ MHz/T is the muon gyromagnetic ratio, B_s and B_{bg} are the respective local fields sensed by implanted muons in the sample and sample holder, ϕ is the initial phase, and σ is a Gaussian relaxation rate. In the superconducting state, the Gaussian relaxation rate includes contributions from both the FLL (σ_{sc}) and a temperature-independent relaxation due to nuclear moments (σ_n). Below T_c, σ_{sc} can be extracted after subtracting σ_n in quadrature,

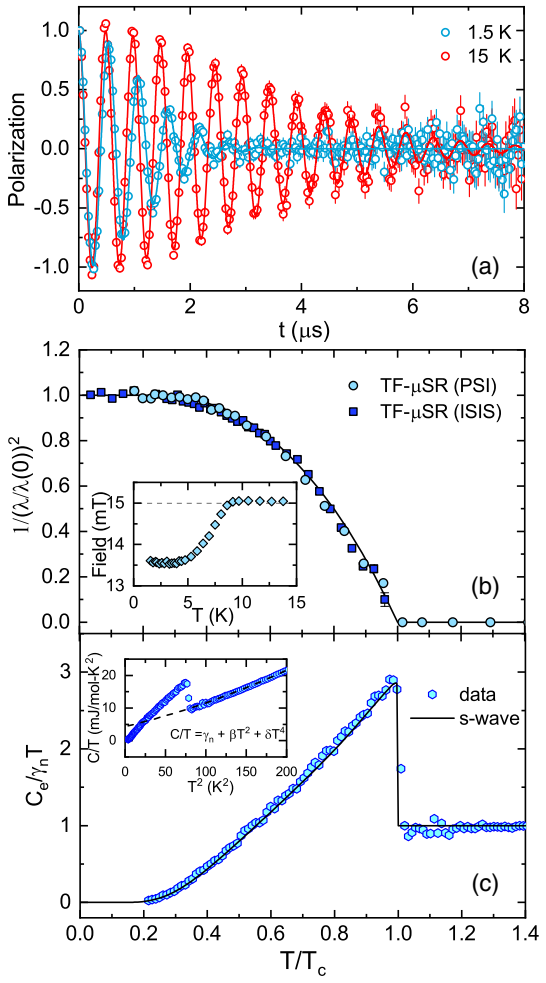

FIG. 2. (a) Time-domain TF-μSR spectra in the superconducting and normal states of $Re_{0.82}Nb_{0.18}$ show very different relaxation rates. (b) Normalized superfluid density vs temperature, as determined from μSR measurements. Inset: temperature dependence of the internal field across T_c. (c) Temperature dependence of the zero-field electronic specific heat. The inset shows the total C/T data versus T^2. The dashed-line is a fit to $C/T = \gamma_n + \beta T^2 + \delta T^4$, used to estimate the phonon contribution. The solid lines in (b) and (c) represent fits using a fully gapped s-wave model.

i.e., $\sigma_{sc} = \sqrt{\sigma^2 - \sigma_n^2}$. Since σ_{sc} is directly related to the magnetic penetration depth and hence the superfluid density, the superconducting gap value and its symmetry can be determined from the measured relaxation rate.

As shown in the inset of Fig. 2(b), a clear diamagnetic shift appears below T_c. At the same temperature, the formation of the FLL is apparent from the rapid increase of σ_{sc}, in turn reflecting an increase of the superfluid density. For small applied magnetic fields [$H_{appl}/H_{c2} \ll 1$], the effective penetration depth λ_{eff} can be calculated from [32,33]:

$$\frac{\sigma_{sc}^2(T)}{\gamma_\mu^2} = 0.00371 \frac{\Phi_0^2}{\lambda_{eff}^4(T)}. \quad (1)$$

Figure 2(b) shows the normalized superfluid density ($[\lambda(T)/\lambda(0)]^{-2}$) vs the reduced temperature T/T_c for $Re_{0.82}Nb_{0.18}$. Clearly the temperature dependence of the superfluid density is highly consistent between PSI and ISIS, and well described by an s-wave model with a single gap of 1.61(1) meV. By using the 15-mT data, the resulting $\lambda(0)$ of 357(3) nm is comparable with 352(3) nm, the value calculated from $\mu_0 H_{c1}$ [24]. The superconducting gap is similar to that of other ReT superconductors, e.g., Re_6Zr (1.21 meV) [15,34], $Re_{24}Ti_5$ (1.08 meV) [18], Re_6Ti (0.95 meV) [17], and Re_6Hf (1.10 meV) [16,35,36], (see also Table SI in the Supplemental Material) [24]. Also, the $2\Delta/k_B T_c$ values of these compounds [e.g., 4.26 for $Re_{0.82}Nb_{0.18}$] are higher than 3.53, the value expected for weakly-coupled BCS superconductors, thus indicating a moderately strong electron-phonon coupling in these materials. The superconducting parameters of all these α-Mn-type ReT NCSC are summarized in Table SI in the Supplemental Material [24].

A detailed analysis of the zero-field specific-heat data provides further insight into the superconducting properties of $Re_{0.82}Nb_{0.18}$. The electronic specific heat C_e/T was obtained by subtracting the phonon contribution from the experimental data [24]. The derived C_e/T was then divided by the normal-state electronic specific heat coefficient, as shown in the main panel as a function of T/T_c. The solid line in Fig. 2(c) represents a fit with $\gamma_n = 4.4$ mJ mol^{-1} K^{-2} and a single isotropic gap $\Delta(0) = 1.52(2)$ meV. This reproduces the experimental data very well, while being consistent with the TF-μSR [see Fig. 2(b)] and previously reported values [37,38]. Note also that this value is between the two values found from a two-gap analysis [39]. The specific-heat jump at T_c was found to be $\Delta C/\gamma_n T_c \sim 1.94$, i.e., larger than the conventional BCS value of 1.43, again indicating a moderately enhanced electron-phonon coupling in $Re_{0.82}Nb_{0.18}$.

The key goal of the present Letter is to probe a possible TRSB in $Re_{0.82}Nb_{0.18}$ and in pure Re. To this aim, we performed detailed zero-field muon-spin relaxation (ZF-μSR) measurements. Normally, in the absence of external fields, the onset of superconductivity does not imply changes in the ZF-μSR relaxation rate. However, in the presence of TRSB, the onset of a tiny spontaneous polarization or currents gives rise to associated (weak) magnetic fields, readily detected by ZF-μSR as an increase in the μSR relaxation rate. Given the tiny size of such effects, we measured the ZF-μSR, both above T_c and inside the superconducting phase. Representative ZF-μSR spectra collected above and below T_c for $Re_{0.82}Nb_{0.18}$ and Re show measurable differences [see Figs. 3(a)–3(b)]. To exclude the presence of stray magnetic fields, all magnets were quenched before the measurements and an active compensation system was used. In nonmagnetic materials in the absence of applied fields, the relaxation is determined primarily by the randomly oriented nuclear dipole

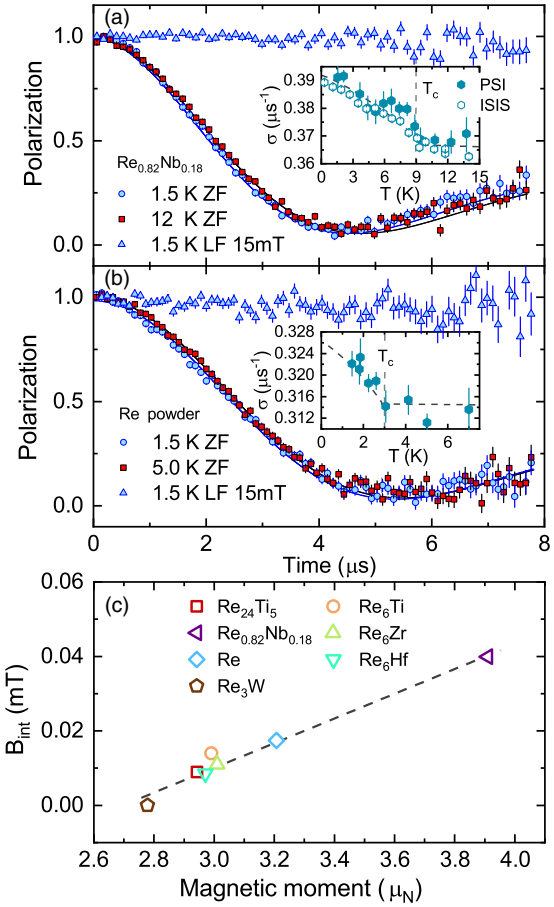

FIG. 3. Representative zero-field μSR spectra for (a) $Re_{0.82}Nb_{0.18}$ and (b) pure Re metal in the superconducting and normal states. Additional μSR data sets collected at 1.5 K in a 15-mT longitudinal field, are also shown. The solid lines are fits using Eq. (2). Insets show the T-dependence of the relaxation rate σ. The results from ISIS in (a) were obtained by fitting the ZF data with the corresponding expression in Ref. [15]. (c) Calculated internal field vs nuclear magnetic moment for ReT superconductors. For the pure Re (diamond), the value was obtained by an extrapolation to 0 K. The reported data are from Refs. [15–18,34–36,42]. The dashed-line indicates a linear behavior. The nuclear moment was estimated from the respective nuclear moments $\mu_{n,\mathrm{Re}}$, $\mu_{n,\mathrm{T}}$ and chemical fractions f_{Re} and f_{T} of Re and T using $\mu_n = \sqrt{f_{\mathrm{Re}}\mu_{n,\mathrm{Re}}^2 + f_{\mathrm{T}}\mu_{n,\mathrm{T}}^2}$.

moments, normally described by a Gaussian Kubo-Toyabe relaxation function [40,41]. In our case, the ZF-μSR spectra are well described by a combined Lorentzian and Gaussian Kubo-Toyabe relaxation function:

$$P_{\mathrm{CKT}} = P_s\left[\frac{1}{3}+\frac{2}{3}(1-\sigma^2t^2-\Lambda t)e^{[-(\sigma^2t^2/2)-\Lambda t]}\right]+P_{\mathrm{bg}}. \quad (2)$$

Here, P_s and P_{bg} are the same as in the TF-μSR spectra. As shown in the insets of Fig. 3, despite the different T_c values of $Re_{0.82}Nb_{0.18}$ and Re, their $\sigma(T)$ curves exhibit a small yet *distinct increase* below T_c, similar to that found also in other ReT NCSC [15–18]. At the same time, the Lorentzian relaxation rate $\Lambda(T)$ remains mostly constant in the studied temperature range, with typical values of 0.007 and 0.005 μs^{-1} for $Re_{0.82}Nb_{0.18}$ and Re [24], respectively, indicating that fast-fluctuation effects are absent in these systems. The small, yet measurable increases of $\sigma(T)$ below T_c, detected from measurements at both facilities, reflect the onset of spontaneous magnetic fields, and thus, they are signatures of TRSB in the superconducting phases of both $Re_{0.82}Nb_{0.18}$ and Re. Further refinements performed by fixing the Λ values gave similarly robust features in $\sigma(T)$ [24]. To rule out the possibility of a defect- or impurity-induced relaxation at low temperatures, we performed auxiliary longitudinal-field μSR measurements at 1.5 K. As shown in Figs. 3(a)–3(b), a small field of 15 mT is sufficient to decouple the muon spins from the weak spontaneous magnetic fields in both samples, indicating that the relevant fields are static on the time scale of the muon lifetime.

To date, most α-Mn-type ReT-NCSC have been found to exhibit TRSB in the superconducting state [15–18]. Our results show that $Re_{0.82}Nb_{0.18}$ is not just another member of the ReT-NCSC family, but one with the most distinct TRSB in the superconducting state (i.e., with the highest σ_{int}, which represents the change of muon relaxation rate between the normal and superconducting states (see details in Table SI in Supplemental Material) [24]. This is clearly depicted in Fig. 3(c), where we plot the estimated internal field B_{int} as a function of the nuclear magnetic moment μ_n for the ReT-NCSC. It can be seen that, B_{int} ($\propto \sigma_{\mathrm{int}}$) scales linearly with μ_n, reaching 0.038 mT for $Re_{0.82}Nb_{0.18}$. At the other extreme, the line crosses the horizontal axis at $\mu_n \sim 2.7\mu_N$, where σ_{int} drops below the resolution of the μSR technique (0.01 mT). This is exactly the case for Re_3W, whose σ_{int} turned out to be negligible [42].

Having detected TRSB in Re-based superconductors still leaves open the most intriguing question: what is its key ingredient? In ReT, the replacement of heavy 5d elements, such as Hf, with lighter 3d elements, such as Ti, appears to have a negligible effect on TRSB. The insensitivity of TRSB to the specific transition-metal element T suggests that a substitution at the T-sites does not significantly influence it. This is confirmed by the persistence of TRSB in elemental Re. In addition, this indicates also that a lack of inversion symmetry is inessential. Finally, there is no TRSB in the superconducting states of $Mg_{10}Ir_{19}B_{16}$ [43] and $Nb_{0.5}Os_{0.5}$ [44], two NCSCs isostructural to ReT and with similar SOC strengths. The above considerations strongly suggest that it is the *local electronic structure* of Re that is crucial for understanding the TRSB in the superconducting states of Re and ReT. To reinforce the above conclusion, one could study other Re-free materials with the α-Mn-type structure. TaOs, with a bulk T_c of

2.07 K and the required crystal structure, represents a good example [45].

We now discuss the possible symmetries of the superconducting order parameter. In the limit of weak SOC, TRSB can be achieved via nonunitary triplet pairing, as, e.g., in $LaNiC_2$ [46] and $LaNiGa_2$ [47,48]. More generally, the relationship between TRSB and triplet pairing is quite complex. For example, the admixed triplet component in so-called "*s*-wave" NCSC (those whose superconducting instabilities do not break crystal point-group symmetries), such as Li_2Pt_3B, does not show TRSB [5]. Conversely, there are TRSB states not involving triplet pairing, e.g., the $s + id$ singlet state proposed for some iron-based superconductors [49]. Apart from the weak-SOC nonunitary triplet pairing scenario mentioned above [46,47], the essential requirement for TRSB occurrence is that the point group of the crystal has irreducible representations with dimension $D > 1$.

The point groups T_d and D_{6h} relevant to ReT and Re, respectively, have several irreducible representations with $D = 2$ or 3. Therefore, they can support TRSB states with singlet-, triplet-, or in the case of ReT, admixed pairing, independent of SOC strength. In what follows, we will assume strong SOC. The full symmetry analysis and plots of the possible order parameters can be found in the Supplemental Material [24]. For ReT there are a number of possible TRSB states, with some examples of pairing functions being given in Ref. [15]. However, all of the possible states have symmetry-constrained point or line nodes, inconsistent with the experimental observations. In view of this, in some systems, it has been proposed that a full gap may be obtained through a Loop-Josephson-Current (LJC) state built on site, intraorbital, singlet pairing. Although it has been shown that the crystal symmetry of ReT is compatible with this scenario [50], the energetics that would drive such a state, if realized, and why it would occur only in systems with Re and not other elements, remain unclear.

The symmetry analysis of pure Re contrasts strongly that of ReT. First, Re is centrosymmetric, implying that the superconducting instability can only take place in either purely-singlet or purely-triplet channels (irrespective of the strength of SOC). Second, due to only two distinct symmetry-related sites per unit cell, a LJC state here is not the most natural one [50]. Third, the crystallographic space group is nonsymmorphic, which in principle allows superconducting instabilities that break screw-axis or glide-plane symmetries. Ignoring the ones that break those symmetries, we find two possible TRSB states, one in the singlet channel with a line node at $k_z = 0$, and another in the triplet channel, with two point nodes on the k_z axis (see Supplemental Material [24]). The Fermi surface of Re has five sheets, including an electron sheet centered on the Γ point and open along the k_z axis, and three hole sheets that are closed, centered on the L point, and not intersecting the $k_z = 0$ plane [51]. These would be compatible with a full gap for the triplet and singlet TRSB states, respectively.

In summary, we performed comparative μSR studies of the noncentrosymmetric $Re_{0.82}Nb_{0.18}$ and centrosymmetric Re superconductors. Bulk superconductivity with $T_c = 8.8$ K ($Re_{0.82}Nb_{0.18}$) and 2.7 K (Re) was characterized by magnetic and transport properties. Both the superfluid density and the zero-field specific-heat data reveal a single-gap nodeless superconductivity in $Re_{0.82}Nb_{0.18}$. The spontaneous fields appearing below T_c, which increase with decreasing temperature, provide strong evidence that the superconducting states of both noncentrosymmetric $Re_{0.82}Nb_{0.18}$ and centrosymmetric Re show TRSB and are unconventional. Comparisons with other Re-free α-Mn-type superconductors suggest that in the ReT family, the TRSB is crucially related to the presence of Re, a key idea for understanding the peculiar behavior of ReT superconductors. We have considered the possible symmetries of the order parameter in these systems and their compatibility with the observed fully gapped spectrum. Further theoretical and experimental work on Re is required to clarify the open issues.

This work was supported by the National Natural Science Foundation of China (Grants No. 11874320 and No. 11474251), National Key R&D Program of China (Grants No. 2017YFA0303100 and No. 2016YFA0300202), the Fundamental Research Funds for the Central Universities, and the Schweizerische Nationalfonds zur Förderung der Wissenschaftlichen Forschung (Grants No. 20021-169455 and No. 206021-139082). The work at the University of Warwick was supported by EPSRC UK through Grant No. EP/M028771/1. Experiments at the ISIS Pulsed Neutron and Muon Source were supported by a beamtime allocation from STFC. S. K. G. and J. Q. are supported by EPSRC through the project "Unconventional Superconductors: New paradigms for new materials" (Grant No. EP/P00749X/1).

*Corresponding author.
tian.shang@psi.ch
†Corresponding author.
msmidman@zju.edu.cn
‡Corresponding author.
j.quintanilla@kent.ac.uk
§Corresponding author.
tshiroka@phys.ethz.ch
‖On leave from Institute of Physics, Polish Academy of Sciences, Aleja Lotnikow 32/46. PL-02-668 Warsaw, Poland.

[1] In *Non-Centrosymmetric Superconductors*, edited by E. Bauer and M. Sigrist (Springer Verlag, Berlin, 2012), Vol. 847.
[2] M. Smidman, M. B. Salamon, H. Q. Yuan, and D. F. Agterberg, Rep. Prog. Phys. **80**, 036501 (2017).

[3] I. Bonalde, W. Brämer-Escamilla, and E. Bauer, Phys. Rev. Lett. **94**, 207002 (2005).

[4] H. Mukuda, T. Fujii, T. Ohara, A. Harada, M. Yashima, Y. Kitaoka, Y. Okuda, R. Settai, and Y. Onuki, Phys. Rev. Lett. **100**, 107003 (2008).

[5] H. Q. Yuan, D. F. Agterberg, N. Hayashi, P. Badica, D. Vandervelde, K. Togano, M. Sigrist, and M. B. Salamon, Phys. Rev. Lett. **97**, 017006 (2006).

[6] M. Nishiyama, Y. Inada, and G.-q. Zheng, Phys. Rev. Lett. **98**, 047002 (2007).

[7] G. M. Pang, M. Smidman, W. B. Jiang, J. K. Bao, Z. F. Weng, Y. F. Wang, L. Jiao, J. L. Zhang, G. H. Cao, and H. Q. Yuan, Phys. Rev. B **91**, 220502 (2015).

[8] D. T. Adroja, A. Bhattacharyya, M. Telling, Y. Feng, M. Smidman, B. Pan, J. Zhao, A. D. Hillier, F. L. Pratt, and A. M. Strydom, Phys. Rev. B **92**, 134505 (2015).

[9] J. Chen, L. Jiao, J. L. Zhang, Y. Chen, L. Yang, M. Nicklas, F. Steglich, and H. Q. Yuan, New J. Phys. **15**, 053005 (2013).

[10] S. Kuroiwa, Y. Saura, J. Akimitsu, M. Hiraishi, M. Miyazaki, K. H. Satoh, S. Takeshita, and R. Kadono, Phys. Rev. Lett. **100**, 097002 (2008).

[11] E. Bauer, G. Hilscher, H. Michor, C. Paul, E. W. Scheidt, A. Gribanov, Y. Seropegin, H. Noël, M. Sigrist, and P. Rogl, Phys. Rev. Lett. **92**, 027003 (2004).

[12] E. M. Carnicom, W. W. Xie, T. Klimczuk, J. J. Lin, K. Górnicka, Z. Sobczak, N. P. Ong, and R. J. Cava, Sci. Adv. **4**, eaar7969 (2018).

[13] A. D. Hillier, J. Quintanilla, and R. Cywinski, Phys. Rev. Lett. **102**, 117007 (2009).

[14] J. A. T. Barker, D. Singh, A. Thamizhavel, A. D. Hillier, M. R. Lees, G. Balakrishnan, D. M. Paul, and R. P. Singh, Phys. Rev. Lett. **115**, 267001 (2015).

[15] R. P. Singh, A. D. Hillier, B. Mazidian, J. Quintanilla, J. F. Annett, D. M. Paul, G. Balakrishnan, and M. R. Lees, Phys. Rev. Lett. **112**, 107002 (2014).

[16] D. Singh, J. A. T. Barker, A. Thamizhavel, D. M. Paul, A. D. Hillier, and R. P. Singh, Phys. Rev. B **96**, 180501 (2017).

[17] D. Singh, K. P. Sajilesh, J. A. T. Barker, D. M. Paul, A. D. Hillier, and R. P. Singh, Phys. Rev. B **97**, 100505 (2018).

[18] T. Shang, G. M. Pang, C. Baines, W. B. Jiang, W. Xie, A. Wang, M. Medarde, E. Pomjakushina, M. Shi, J. Mesot, H. Q. Yuan, and T. Shiroka, Phys. Rev. B **97**, 020502 (2018).

[19] G. M. Luke, Y. Fudamoto, K. M. Kojima, M. I. Larkin, J. Merrin, B. Nachumi, Y. J. Uemura, Y. Maeno, Z. Q. Mao, Y. Mori, H. Nakamura, and M. Sigrist, Nature (London) **394**, 558 (1998).

[20] Y. Aoki, A. Tsuchiya, T. Kanayama, S. R. Saha, H. Sugawara, H. Sato, W. Higemoto, A. Koda, K. Ohishi, K. Nishiyama, and R. Kadono, Phys. Rev. Lett. **91**, 067003 (2003).

[21] J. Xia, Y. Maeno, P. T. Beyersdorf, M. M. Fejer, and A. Kapitulnik, Phys. Rev. Lett. **97**, 167002 (2006).

[22] E. R. Schemm, W. J. Gannon, C. M. Wishne, W. P. Halperin, and A. Kapitulnik, Science **345**, 190 (2014).

[23] A. Sumiyama, D. Kawakatsu, J. Gouchi, A. Yamaguchi, G. Motoyama, Y. Hirose, R. Settai, and Y. Ōnuki, J. Phys. Soc. Jpn. **84**, 013702 (2014).

[24] See the Supplemental Material at http://link.aps.org/supplemental/10.1103/PhysRevLett.121.257002 for details on the measurements of crystal structure, heat capacity, electrical resistivity, and critical field, as well as for the data analysis and the symmetry-allowed TRSB order parameters, which includes Refs. [25–30].

[25] N. R. Werthamer, E. Helfand, and P. C. Hohenberg, Phys. Rev. **147**, 295 (1966).

[26] T. Klimczuk, Q. Xu, E. Morosan, J. D. Thompson, H. W. Zandbergen, and R. J. Cava, Phys. Rev. B **74**, 220502 (2006).

[27] P. K. Biswas, M. R. Lees, A. D. Hillier, R. I. Smith, W. G. Marshall, and D. M. Paul, Phys. Rev. B **84**, 184529 (2011).

[28] A. Tari, *The Specific Heat of Matter at Low Temperatures* (Imperial College Press, London, 2003).

[29] T. H. K. Barron and G. K. White, *Heat Capacity and Thermal Expansion at Low Temperatures* (Kluwer, New York, 1999).

[30] R. Waterstrat and R. Manuszewski, J. Less-Common Met. **51**, 55 (1977).

[31] G. B. Balakrishnan, M. Smidman, A. D. Hillier, and D. M. Paul, Experiment No. RB1120180, STFC ISIS Facility, (2011), DOI: 10.5286/ISIS.E.24088309.

[32] W. Barford and J. M. F. Gunn, Physica (Amsterdam) **156C**, 515 (1988).

[33] E. H. Brandt, Phys. Rev. B **68**, 054506 (2003).

[34] D. A. Mayoh, J. A. T. Barker, R. P. Singh, G. Balakrishnan, D. M. Paul, and M. R. Lees, Phys. Rev. B **96**, 064521 (2017).

[35] D. Singh, A. D. Hillier, and A. Thamizhavel, Phys. Rev. B **94**, 054515 (2016).

[36] B. Chen, Y. Guo, H. Wang, Q. Su, Q. Mao, J. Du, Y. Zhou, J. Yang, and M. Fang, Phys. Rev. B **94**, 024518 (2016).

[37] J. Chen, L. Jiao, J. L. Zhang, Y. Chen, L. Yang, M. Nicklas, F. Steglich, and H. Q. Yuan, Phys. Rev. B **88**, 144510 (2013).

[38] A. B. Karki, Y. M. Xiong, N. Haldolaarachchige, S. Stadler, I. Vekhter, P. W. Adams, D. P. Young, W. A. Phelan, and J. Y. Chan, Phys. Rev. B **83**, 144525 (2011).

[39] C. Cirillo, R. Fittipaldi, M. Smidman, G. Carapella, C. Attanasio, A. Vecchione, R. P. Singh, M. R. Lees, G. Balakrishnan, and M. Cuoco, Phys. Rev. B **91**, 134508 (2015).

[40] R. Kubo and T. Toyabe, in *Magnetic Resonance and Relaxation*, edited by R. Blinc (North-Holland, Amsterdam, 1967).

[41] A. Yaouanc and P. D. de Réotier, *Muon Spin Rotation, Relaxation, and Resonance: Applications to Condensed Matter* (Oxford University Press, Oxford, 2011).

[42] P. K. Biswas, A. D. Hillier, M. R. Lees, and D. M. Paul, Phys. Rev. B **85**, 134505 (2012).

[43] A. A. Aczel, T. J. Williams, T. Goko, J. P. Carlo, W. Yu, Y. J. Uemura, T. Klimczuk, J. D. Thompson, R. J. Cava, and G. M. Luke, Phys. Rev. B **82**, 024520 (2010).

[44] D. Singh, J. A. T. Barker, T. Arumugam, A. D. Hillier, D. M. Paul, and R. P. Singh, J. Phys. Condens. Matter **30**, 075601 (2018).

[45] D. Singh, K. P. Sajilesh, S. Marik, A. D. Hillier, and R. P. Singh, Supercond. Sci. Technol. **30**, 125003 (2017).

[46] J. Quintanilla, A. D. Hillier, J. F. Annett, and R. Cywinski, Phys. Rev. B **82**, 174511 (2010).
[47] A. D. Hillier, J. Quintanilla, B. Mazidian, J. F. Annett, and R. Cywinski, Phys. Rev. Lett. **109**, 097001 (2012).
[48] Z. F. Weng, J. L. Zhang, M. Smidman, T. Shang, J. Quintanilla, J. F. Annett, M. Nicklas, G. M. Pang, L. Jiao, W. B. Jiang, Y. Chen, F. Steglich, and H. Q. Yuan, Phys. Rev. Lett. **117**, 027001 (2016).
[49] W.-C. Lee, S.-C. Zhang, and C. Wu, Phys. Rev. Lett. **102**, 217002 (2009).
[50] S. Ghosh, J. F. Annett, and J. Quintanilla, arXiv:1803.02618.
[51] L. F. Mattheiss, Phys. Rev. **151**, 450 (1966).